Netsu Sokutei **39**(2), 41-46 (2012)

Article

Variable Temperature AFM Observation of Phase Separation in NR/BR Blend

Yoshihisa Inoue[a, c], Masayuki Iwasa[b], and Hirohisa Yoshida[a]*
[a]Graduate School of Urban Environmental Science, Tokyo Metropolitan University,
1-1, Minamiosawa, Hachiouji, Tokyo, 192-0397 Japan,
[b]SII NanoTechnology Inc., 2-15-5 RBM Tsukiji Building,
Shintomi, Chuo-ku, Tokyo,104-0041 Japan,
[c]Yokohama Rubber Co. Ltd., 2-1 Oiwake, Hiratsuka, Kanagawa, 254-0014, Japan
*yoshida-hirohisa@tmu.ac.jp

(Received, Oct. 16, 2011; Accepted, Dec. 1, 2011)

The phase images of natural rubber / poly(butadiene) (NR/BR) blend were observed at various temperatures by the dynamic force mode AFM at 370 Hz. The phase separated structure of NR/BR blend was observed in the temperature range between -70 and 30 ^{o}C, which corresponded to rubbery BR and glassy NR phases. The phase separated structure scarcely changed with temperature, however the phase contrast between BR and NR phases changed with temperature. The phase angle difference of NR and BR domains which was normalized by the phase angle of ZnO, shifted continuously with temperature. The glass transition temperatures (*T*g) of each domain were obtained from the temperature dependency of the phase angle difference. The relationship between the frequency and the reciprocal *T*g values, which were evaluated by AFM (370 kHz), dynamic mechanical analysis (2 – 10 Hz) and dielectric relaxation spectroscopy (10^2 – 10^5 Hz), showed Vogel-Fulcher relationship.

Keywords: atomic force microscopy, phase image, phase separation, NR/BR blend, glass transition

1. Introduction

Elastomer blends are widely used in industry, natural rubber / poly(butadiene) (NR/BR) blend is one of typical combination for rubber industry. For instance, NR/BR is used in tread and side wall part of tire for automobile because of its high strength, wear resistance and anti-fatigue to failure ability. Many researches of NR/BR started from 1960's, it was reported that NR/BR blend was immiscible by dynamic mechanical analysis (DMA) and dielectric relaxation spectroscopy (DES).[1)] Differential Scanning Calorimetry (DSC) and DMA are popular methods to evaluate the miscibility of polymer blends, however those information (transition temperature, glass transition temperature, specific heat, modulus, loss modulus etc.) are the average properties of blend system.

With the improvement of instruments, however, the intermediate phase of NR/BR blend was observed by a temperature modulated differential scanning calorimeter (TM-DSC) and NR/BR was considered as a partially miscible system.[2)] Hess *et al*[3)] reported the phase separated structure of NR/BR by a transmission electron microscope (TEM), the domain size of NR/BR was from submicron to micron order. In order to observe soft samples by TEM, samples are mounted hard materials such as poly(methyl methacrylate), and then a mounted sample is cut to ultra-thin sections by microtome. The staining by heavy ions such as osmium is ordinal method for TEM observation of organic and polymeric materials.[4, 5)] These sample preparation disturb to observe the original phase separated structure of samples, due to the swelling by MMA monomer and the staining. The phase separated structure of polymer blends are also investigated by small angle scattering method using light, X-ray (SAXS) and neutron (SANS).[6,7)] The spinodal decomposition process of poly(isoprene)/BR system is successful analyzed by scaling law.[8)] The phase separation of NR/BR blend has too small electron density difference to evaluate by SAXS, and the deuterated sample is required for SANS.

Rubber compounds consist of several polymers and inorganic materials to satisfy the required performance. As the heterogeneous phase separated structure of polymer blends and inorganic materials in rubber compounds are nanometer order, the analysis of structure and physical property in nano-scale are required. TEM and Atomic Force Microscope (AFM) are used to observe nano-scale morphology of polymer blends.[9-14)] In recently, many studies of phase separated structure by AFM are reported, because of higher resolution of surface structure, information of molecular motion and easy sample preparation.

There are two modes of AFM measurement, contact and non-contact modes. In contact mode, a tip of cantilever contacts to sample surface directly and slides to horizontal direction to obtain frictional force of sample surface. Dynamic modulus and adhesive force of target area of sample are obtained by the deformation of cantilever during approach and release process by forth curve analysis.[15)] The surface of soft materials takes mechanical damages by a cantilever tip easily in the contact mode. The friction force between a tip and sample surface is influenced by the surface roughness. Rubber products consisted of soft compounds contain many hard particles, such as zinc oxide and carbon black, have essentially a rough surface. Therefore, it is difficult to observe the rubber surface by the contact mode.

The non-contact mode (dynamic force mode, DFM) can observe topographic and phase images from amplitude and phase changes caused by interaction between sample surface and cantilever tip oscillating at around its resonance frequency. The phase image includes many information such as hardness, viscoelasticity and adhesion reflecting molecule motion of sample,[16-19] these information are influenced by surface roughness, inclination, shape of probe tip and driving amplitude.[20,21] Therefore, the observed phase images include not only the real space image of sample surface but also the artifacts caused by the various factors. As the phase image obtained by DFM include the molecular motion of sample surface, this method is suitable for the soft materials having rough surface such as rubber compounds.

Many researchers investigated glass transition behavior of polymer blends by contact mode evaluating friction force [22,23] and adhesion force [24,25] at various temperatures. Dynamic modulus (*E'*) obtained by AFM indicates the similar value obtained by DMA (24). For the multiple blend system consisted of components having different glass transition temperature (*T*g), the AFM phase image will give the different images at various temperatures. In this study, the phase separation structure of NR/BR blend prepared by industrial procedure was observed by AFM with DFM at various temperatures in order to evaluate the phase separate structure and the molecular motion of each phase separated domain.

2. Samples and Experiments

2.1 Samples

The elastomers used in this study were natural rubber (NR), poly-butadiene (BR) and these blend NR/BR. NR was RSS#4 (ribbed smoked sheet #4) produced in Thailand and BR was Nipole 1220 supplied from ZEON Co. Ltd., Japan, with high cis-1,4 poly-butadiene content (97%) and weight-average molecular weight of 470,000 g/mol.

The recipe and cure condition of NR/BR blend (NR/BR = 60/40 in mass ratio) were listed in **Table 1**. The elastomers, stearic acid and zinc oxide were mixed by a lab scale roll mill for 6 min at 70 °C. The other remaining chemicals were added and mixed continued for additional 6 min. After the 12 min mixing process, the uncured NR/BR compound was removed from the roll mill and sheeted (1 mm thickness). Then, NR/BR compound was placed in a press mold and cured for 15 min at 160 °C.

Table 1 Recipe of NR, NR/BR and BR vulcanizes

Component	NR(100)	NR/BR(60/40)	BR(100)
NR*[a]	100	60	0
BR*[b]	0	40	100
ZnO (phr)*[c]	3.5	3.5	3.5
Stearic Acid (phr)	2	2	2
Sulfur (phr)	2	2	2
TBBS*[d] (phr)	1	1	1

Cure condition: 160 °C/15 min.
*a Ribbed smoked sheet #4
*b Nippol 1220, High cis polybutadiene rubber
*c Per hundred rubber
*d N-tertiary butyl benzothiazyl sulfenamide

2.2 Atomic Force Microscopy (AFM)

AFM observation was performed by dynamic force mode using E-sweep (SII Nanotechnology Inc., Japan) scanning probe microscope. Topographic (height) and phase images were recorded simultaneously under reduced pressure at various temperatures from -70 to 30 °C. Commercial silicon cantilever probes (SII Nanotechnology Inc.) were used to collect AFM images of the blend systems. Manufacture nominal values for the tip radius, length, and spring constant of the cantilever were 10 nm, 125 μm, and 40 N/m, respectively. During the phase imaging, the cantilever probe tip was oscillated at 370 kHz, which was slightly higher its resonance frequency. The cross section of cured NR/BR for AFM observation was prepared by cutting using a razor.

NR/BR blend was cooled to -70 °C from room temperature at 1 °C min^{-1}, and then AFM observation was carried out at various temperatures from -70 to 30 °C. The sample was heated to each 5 °C steps at 1 °C min^{-1}, and hold at a fixed temperature for 5 min and AMF observation was carried out under isothermal conditions. The time resolution of AFM observation at 6 μm x 6 μm area was 14 mins.

2.3 Differential Scanning Calorimetry (DSC)

DSC measurements of the original NR, BR and the cured NR/BR were performed by DSC (DSC 7020, SII Nanotechnology Inc.) in the temperature range between -140 and 50 °C equipped with a cooling apparatus. The scanning rates were from 1 to 10 °C min^{-1} under the dry nitrogen atmosphere. Temperature and enthalpy calibrations were used the melting temperature and enthalpy of pure indium and mercury.

The glass transition temperature (T_g) was evaluated by the midpoint temperature, where a half of the heat capacity difference between the glassy and the rubbery states (ΔC_p) was obtained on heating. The on-set temperature was employed as the crystallization and melting temperatures both on heating and cooling.

2.4 Dynamic Mechanical Analysis (DMA)

DMA measurements were performed with Rheolograph – solid (Toyoseiki Co. Ltd., Japan) in the temperature range between -100 and 60 °C, at heating rate of 5 °C min^{-1}. The frequencies were 2, 5, 10 Hz, by the extension mode under the 10 % static and 2 % dynamic deformations. The sample size was 1 (thickness) x 5 (width) x 60 (length) mm.

2.5 Dielectric Relaxation Spectroscopy (DES)

DES measurement was carried out at 10^2, 10^3, 10^4 and 10^5 Hz by DES 100U (SII Nanotechnology). The measurement covered the temperature range from -155 to 23 °C at heating rate of 1.25 °C min^{-1}. The sample size for DES measurement was 50 mm in diameter and 0.5 mm thickness.

3. Results and Discussion

3.1 Thermal properties

DSC cooling and heating curves of NR, BR and NR/BR blend at 5 °C min^{-1} were shown in **Fig.1**. NR showed the glass transition (T_g; -64.5 °C, ΔC_p; 0.315 J g^{-1}) on cooling and showed the glass transition (T_g; -62.8 °C, ΔC_p; 0.320 J g^{-1}) accompanying the small endothermic peak due to the enthalpy relaxation on heating at 5 °C min^{-1}. BR showed the broad exothermic peak at around -60 °C due to the crystallization (T_c; -50.3 °C, $\Delta_c H$; 16.9 J g^{-1}) on cooling. BR prepared by cooling from room temperature to -140 °C at 5 °C min^{-1} showed the glass transition (T_g; -103.1 °C, ΔC_p; 0.149 J g^{-1}), the cold-crystallization (T_{cc}; -77.2 °C, $\Delta_{cc} H$; 4.58 J g^{-1}) and the melting (T_m; -44.0 °C, ΔmH; 22.1 J g^{-1}) on heating at 5 K min^{-1}. The summation of crystallization enthalpy observed on cooling and heating ($\Delta_c H$ and $\Delta_{cc} H$) was almost the same with the melting enthalpy (Δ_mH).

NR/BR showed the exothermic peak at -48.1 °C ($\Delta_c H$ normalized by BR weight fraction; 15.2 J g^{-1}) due to BR crystallization overlapped with the glass transition of NR

component on cooling. On heating, the melting of BR crystallites (T_m; –42.5 °C, Δ_mH normalized by BR weight fraction; 22.0 J g^{-1}) was observed. The values of $\Delta_c H$ evaluated on cooling and $\Delta_m H$ of BR component in NR/BR blend indicated that the cold-crystallization corresponding to 1.6 J g^{-1} occurred on heating in the temperature range overlapped with the glass transition of NR component. The cold-crystallization of BR component disturbed to evaluate the exact ΔC_p value of NR component. The ΔC_p value of NR component was evaluated at various heating rate, and the ΔC_p average value was obtained. For NR/BR blend, two glass transitions were observed for phase separated NR (T_g; –63.8 °C, ΔC_p normalized by NR weight fraction; 0.17 – 0.18 J g^{-1}) and BR (T_g; –91.8 °C, ΔC_p normalized by BR weight fraction; 0.22 J g^{-1}) components. The ΔC_p values of NR and BR components indicated that NR rich miscible phase, the interface between NR and BR phases, existed in NR/BR blend.

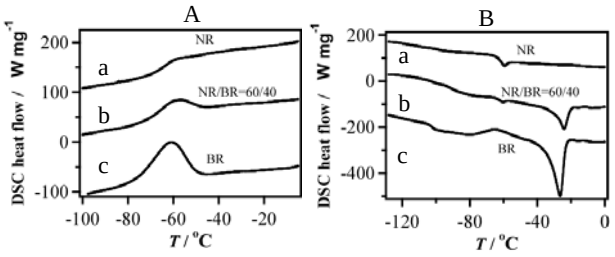

Fig.1 DSC cooling (A) and heating (B) curves of NR (a), BR (c) and NR/BR blend (b) at 5 °C min^{-1}.

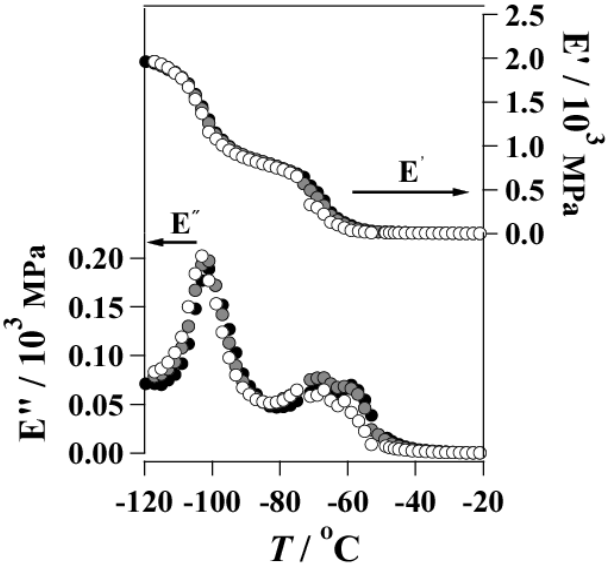

Fig.2 Dynamic mechanical spectra of NR/BR blend at 2, 5, 10 Hz on heating at 5 °C min^{-1}.

Fig.2 shows temperature dispersion of storage modulus (*E*') and loss modulus (*E*") obtained by dynamic mechanical analysis (DMA) of NR/BR blend at 2, 5, 10 Hz on heating. Two main *E*" dispersion peaks were observed around –100 and –60 °C. The dispersion *E*" peak around –60 °C consisted of double peaks. As the glass transition of NR component and the cold-crystallization of BR component occurred in this temperature range at 5 °C min^{-1} by DSC, the *E*" dispersion peak consisted of two modes. From the frequency dependence of *E*" peak temperature, the two peaks appeared at lower and higher temperatures were assigned to glass transition of NR and cold-crystallization of BR, respectively. T_g of BR and NR at 10 Hz determined from *E*" dispersion peak top were –63 and –101 °C, respectively.

Fig.3 shows temperature dispersion of storage dielectric constant (*e*') and loss dielectric constant (*e*") on heating obtained by dielectric relaxation spectroscopy (DES) of NR/BR blend. Two *e*" dispersion peaks corresponding to glass transition of each component were observed. The *e*" peak top temperature was employed as T_g of component. T_g of BR and NR at 100 kHz obtained by DES were –69 and –16 °C, respectively.

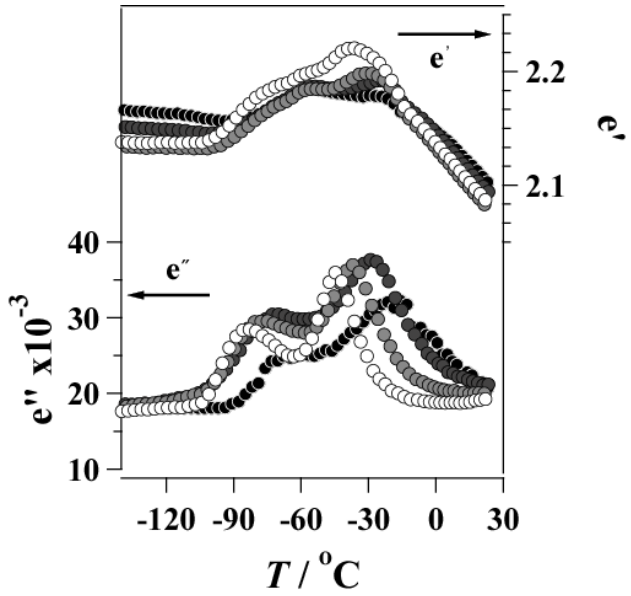

Fig.3 Dielectric relaxation spectra of NR/BR blend at 10^2, 10^3, 10^4 and 10^5 Hz on heating at 1.25 °C min^{-1}.

3.2 AFM phase image

Fig.4 shows AFM phase images of NR/BR blend at various temperatures by dynamic force mode at 370 kHz. NR/BR blend was cooled to –70 °C from room temperature at 1 °C min^{-1}, and AFM observation was started from –70 to 30 °C. Under this experimental condition, the crystallization of BR component occurred on cooling, and a small amount of cold crystallization occurred during heating. The darker part in AFM phase images indicated the harder component. Comparing with the phase images at –70 and 30 °C, the darker image at –70 °C indicated that both NR and BR components were the glassy state. The phase image became brighter with the increase of temperature. For the image at 30 °C, the black spots were zinc oxide (ZnO) particles, which were the hardest materials in NR/BR blend. ZnO particles dispersed heterogeneously as coagulated particles in NR/BR blend, the size and dispersion state of ZnO particles were almost the same even for temperature change.

Both the images at –70 and 30 °C showed no significant phase separated structures. For the phase image at 30 °C showed only the dispersion of ZnO particles, the phase separated structure of NR and BR component was not observed due to the similar hardness of both components, because both components were in the rubber state above their T_g. From the same reason, the phase image at –70 °C showed no clear phase separated structure because both components were in the glassy state. In order to observe the phase separated structure by AFM phase image, the clear difference of hardness between components was necessary, such as one component was the glassy state and the other one was the rubber state. The difference in dynamic modulus between the glassy and the rubber states was about 10^3 Pa from the DMA result for NR/BR blend as shown in **Fig.3**. As T_g of NR component was about 40 °C higher than that of BR

component, the sufficient difference in hardness for AFM phase image observation was obtained in the temperature range between both glass transition temperatures of BR and NR phases.

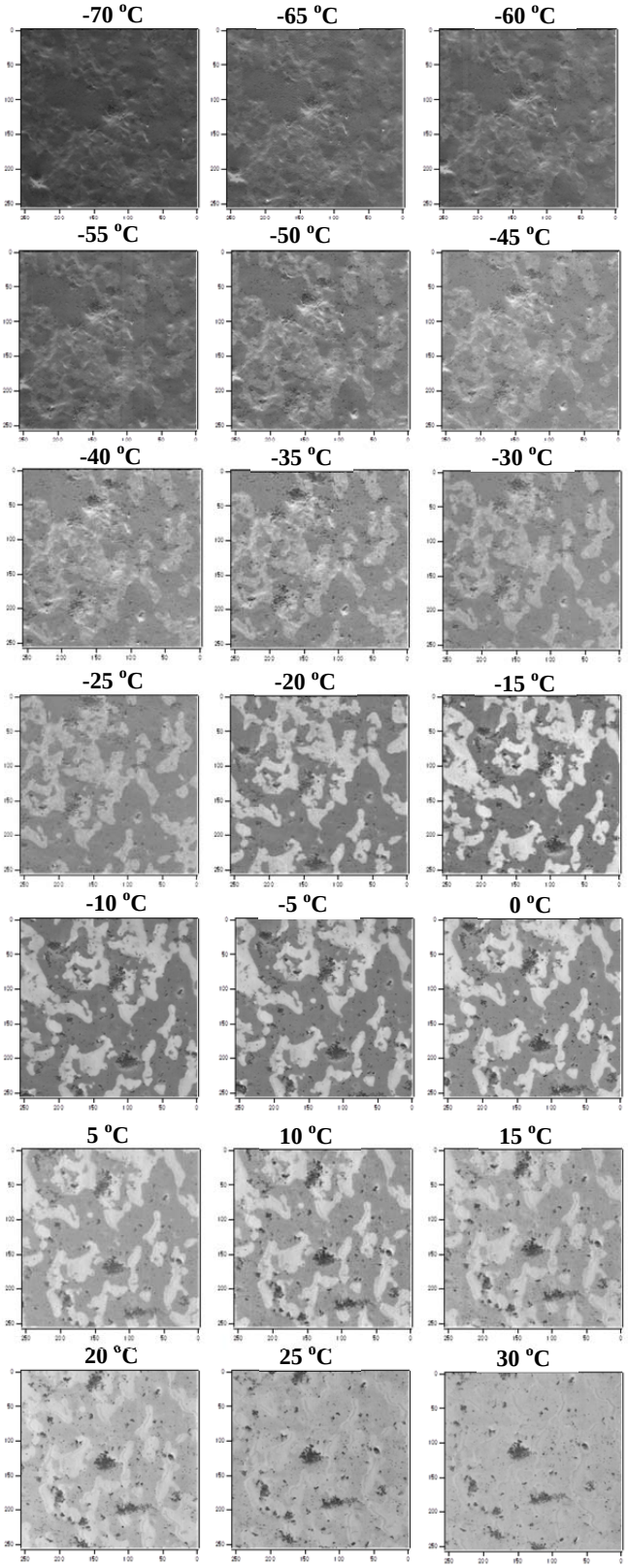

Fig.4 AFM phase images of NR/BR blend at various temperatures from –70 to 30 °C during heating by dynamic force mode at 370 kHz. Scanning area of image was 6 x 6 μm^2.

With increasing temperature, the phase difference appeared above –60 °C, and then the phase separated structure became clear above –40 °C. The BR component changed to the rubber state at lower T_g (–60 °C), however, the NR component remained as the glassy state, therefore, the clear phase difference was observed. The phase separated structure was observed in the temperature range from –60 to 20 °C. The contrast of phase separated structure changed with temperature, however, the shape of structure scarcely changed. The phase separated structure was observed as a result of modulus difference between NR and BR in the different phase. From the area analysis of phase images observed in the temperature range from –60 to 20 °C, the area ratio of darker part was 0.58 to 0.62, which corresponded to the blend ratio of NR.

The phase separated structure became unclear in the phase image at 30 °C, which indicated that the NR domain changed to the rubber state. The phase images obtained in the temperature range between T_g of components gave the phase separated structure without any chemical treatment and complex sample preparations.

It is well known that the phase image is influenced by the surface roughness due to the contact area change of cantilever tip and sample surface. In order to evaluate the effect of surface roughness on the phase images, the height and the phase images of NR/BR blend observed at –20 °C were compared in **Fig. 5**.

The phase separated structure was observed only in the phase image, the height image where the height difference was about 150 nm showed no characteristic structure. The line profiles at the same position in both images were shown in **Fig.5**. The line profile of phase image differed from that of height image. This fact indicated that the phase separated structure observed in the phase image was scarcely affected by the surface roughness of NR/BR blend.

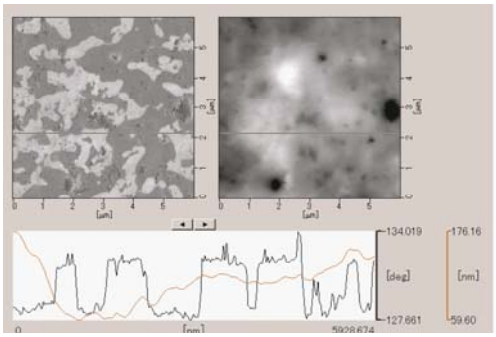

Fig.5 AFM phase (left) and height (right) images of NR/BR blend at -20 °C by dynamic force mode at 370 kHz. Line profiles of phase and height images at the same place (bottom).

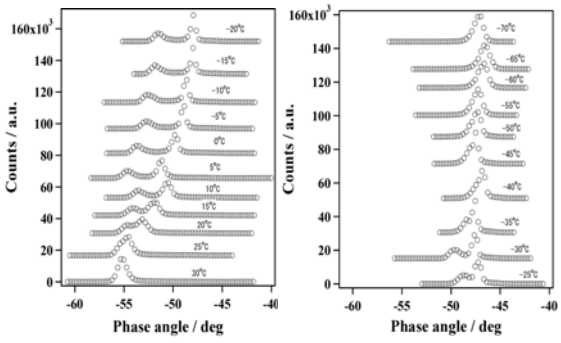

Fig.6 Histogram analysis of AFM phase image observed at various temperatures.

The phase separated structure of NR/BR blend was observed in the temperature range between –60 and 20 °C due to the dynamic modulus difference between NR and BR phase. These AFM results suggested that the glass transition of BR and NR phases occurred at –50 ~ –20 °C and –10 ~ 20 °C, respectively. These T_g values were higher than those observed by DSC, DMA and DES due to the effect of frequency dependence.

In order to evaluate T_g value from the phase image, the numerical analysis of phase image was carried out. The histogram against phase angle at various temperatures evaluated from phase images were shown in **Fig.6**. The phase images were obtained for the same area of NR/BR blend at each temperature, however, the phase value shifted at each measurement process with temperature change. It is difficult to compare the absolute phase angle value at different temperatures in **Fig.6**. The tendency of phase angle changes might be comparable to evaluate the phase image. The peak observed at around –47.5 ° in the phase image in the temperature range between –70 and –20 °C corresponds to the hard component in the phase image. The absolute phase value fluctuated with temperature. However, the peak at around –47.5 ° became broader to the lower phase angle side with increasing temperature, and the shoulder appeared at –35 °C. The shoulder became the independent peak at –35 °C, the peak phase value shifted to the lower phase angle with increasing temperature. Two peaks in the histogram observed in the temperature range between –30 and 20 °C, these two peaks corresponded to the phase separated structure of NR/BR blend. The peak area of histogram indicated the surface area of each domain, the ratio of peak area of higher phase angel to that of lower phase angel was 35/65 which was almost the same with blend ratio.

As the absolute phase angle drifted in each measurement at different temperature, the internal standard is necessary to compensate the phase angle fluctuation. The hardest portion ZnO, which was observed as the black spots in **Fig.4**, was appeared at –44 °, however the portion of ZnO was too low to observe in the histogram shown in **Fig.6**. The phase angles of NR and BR components were subtracted from the phase angle of ZnO, which was used as the internal standard, the normalized phase angle of NR and BR components were plotted as a function of temperature in **Fig.7**.

3.3 Glass transition

The lower phase angle indicated the softer component, that was BR component having lower T_g. The shift of normalized phase angle for both NR and BR components were observed with increasing temperature. The phase angle shift occurred as the result of the interaction change between sample surface and cantilever tip accompanying with glass transition of each component. The middle point temperature of phase angle shift was employed as T_g of each component as shown in **Fig.7**.

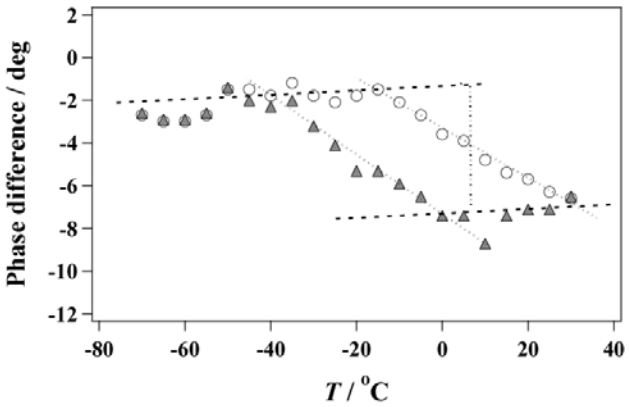

Fig.7 Temperature change of normalized phase angle for BR (solid triangle) and NR (open circle)

The T_g values of NR and BR components observed by AFM phase image, DMA and DES were plotted as a function of measurement frequency in **Fig.8**. The relationship between the reciprocal T_g and logarithm of measurement frequency of NR and BR components was described by Vogel-Fulcher low. This relationship indicated that T_g evaluated from AFM phase image corresponded to T_g at 370 kHz.

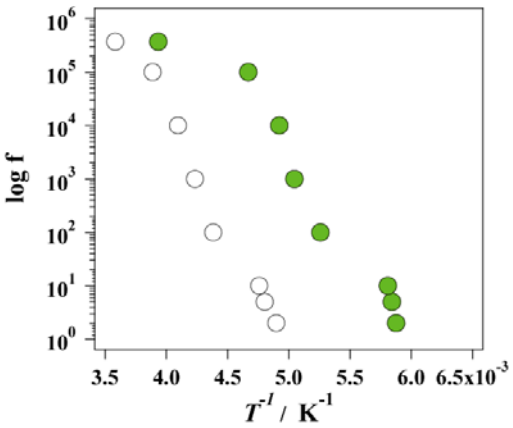

Fig.8 Relationship between reciprocal T_g and measurement frequency of NR (open circle) and BR (solid circle) domains in NR/BR=60/40.

4. Conclusion

The phase separated structure of NR/BR blend was observed by valuable temperature AFM phase image in the temperature range from –70 to 20 °C. AFM phase image indicated the size of soft domain was 200 – 500 nm. The phase angle difference of NR and BR domains, which was normalized by the phase angle of ZnO, changed continuously with temperature. T_g of NR and BR domains were estimated from the temperature change of the normalized phase angle difference of NR and BR domains. T_g of NR and BR domains were obtained by DES at 100 – 100 kHz and by DMA at 2 – 10 Hz. The relationship between the measurement frequency and the reciprocal T_g obtained by AFM, DES and DMA methods showed Vogel-Fulcher relationship. T_g obtained by the temperature valuable AFM phase image was glass transition temperature at 370 kHz.

References

1) K. Fujimoto and N. Yoshimura, *Nippon Gomu Kyoukaishi* **38**(4), 284-288 (1965).
2) D. J. Hourston and M. Song, *J. Appl. Polymer Sci*, **76**(12), 1791-1798 (2000).
3) W. M. Hess, C. E. Scott, Callan, and J. E. Rubber, *Chem. Technol*, **40**, 371-384 (1967).
4) E. H. Andrews, *J. Roy. Microscop. Soc*, **82**, 221-223 (1964).
5) K. Kato, *J. Electron. Microsc*, **14**, 219-220 (1965).
6) S. Koizumi, H. Hasegawa, and T. Hashimoto, *Macromolecules* **27**, 7893-7906 (1994).
7) T. Koga, T. Hashimoto, M. Takenaka, K. Aizawa, N. Amino, M. Nakamura, D. Yamaguchi, and S. Koizumi, *Macromolecules* **41**, 453-464 (2008).
8) M. Takenaka and T. Hashimoto, *J. Chem. Phys*, **96**, 6177-6190 (1992).
9) K. Tanaka, A. Takahara and T. Kajimaya, *Macromolecules* 29, 3232-3239 (1996).

10) A. Takahara, X. Jiang, N. Satomi, K. Tanaka, and T. Kajiyama, *Key. Eng. Mater.* **137**, 79-86 (1998).
11) Y. Li, Y. Yang, F. Yu, and L. Dong, *J. Polym. Sci. Part B: Polym. Phy*. **44**, 9-21 (2005).
12) K. N. Pandey, D. K. Setua, and G. N. Mathur, *Polym. Eng. Sci*. **45**, 1265-1276 (2005).
13) Y. Huang and C. Xiao, *Polymer* **48**, 371-381 (2007).
14) C-H. Lee, J-Y. Liu, S-L. Chen, and Y-Z. Wang, *Polymer J.* **39**, 138-146 (2007).
15) H. Nukaga, S. Fujinami, H. Watabe, K. Nakajima, and T. Nishi, *Jpn. J. Appl. Phys*. **44**, 5425-5429 (2005).
16) S. N. Magonov, V. Elings, and M. Whangbo, *Surf. Sci*. **389**, 201-211 (1997).
17) G. Bar, R. Btandsch, and M. Whangbo. *Surf. Sci. Lett*. **436**, L715-L723 (1999).
18) L. Wang, *Surf. Sci*. **429**, 178-185 (1999).
19) A. Noy, C. H. Sanders, D. V. Vezenov, S. Wong, and C. Lieber, *M. Langmuir* **14**, 1508-1511 (1998).
20) G. Bar, R. Btandsch, and M. Whangbo, *Surf. Sci. Lett*. **422**, L192-L199 (1999).
21) G. Bar, R. Btandsch, and M. Whangbo, *Surf. Sci. Lett*. **411**, L802-L809 (1998).
22) T. Kajiyama, *Korea Polymer Journal* **4**, 186-190 (1996).
23) EL. S Mounir, A. Takahara, and T. Kajiyama, *Polymer Journal* **31**, 89-95 (1999).
24) D. B. Grandy, D. J. Hourston, M. P. Duncan, M. Reading, G. G. Silva, M. Song, and P. A. Syke,. *Macromolecules* **33**, 9348-9359 (2000).
25) B. Cappella and S. Kaliappan, *K. Macromolecules* **39**, 9252-9252 (2006).